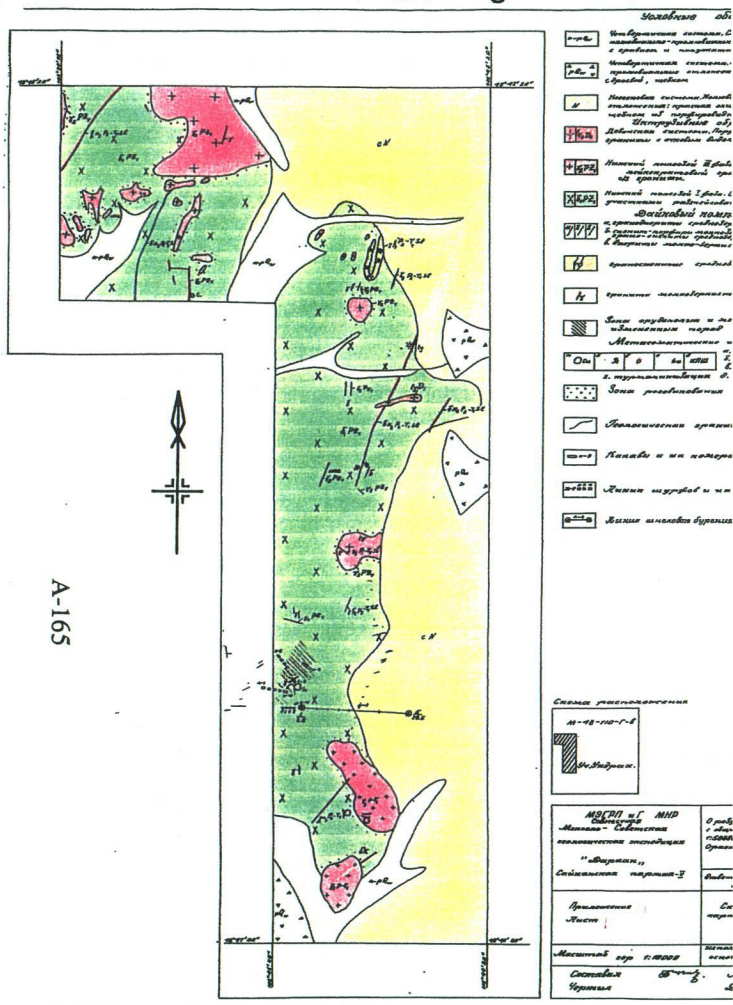


**Appendix 18 Existing data of geological map, geophysical data and  
figures in the Undrakh area**

## A-165



Undrakh area

**Appendix 19 Report on the airborne survey results in the Western  
Erdenet area, Mongolia**

**WESTERN ERDENET AREA  
MONGOLIA**

**Regional Structural Interpretation from Airborne Geophysics and Remote  
Sensing Imagery**

**February, 2002**

## **Table of Contents**

Executive Summary.....	iii
1 INTRODUCTION .....	1
1.1 Objectives and Products.....	3
2 METHODOLOGY AND DATA .....	4
2.1 Airborne Magnetic Data.....	4
2.1.1 Image Processing – Magnetic Data.....	5
2.1.2 Influences on Airborne Magnetic Data .....	8
2.1.3 Uses of Airborne Magnetic Data .....	9
2.2 Airborne Gamma-ray Spectrometer Data .....	10
2.2.1 Image Processing – Gamma-ray Spectrometer Data .....	11
2.2.2 Influences on Airborne Gamma-ray Spectrometry.....	12
2.2.3 Uses of AGRS Data .....	13
2.3 Landsat TM .....	15
3 GEOLOGY REVIEW.....	16
4 INTERPRETATION RESULTS .....	19
4.1 Litho-structural Domains.....	19
4.2 Prospects .....	25
4.2.1 Erdenetiin Ovoo .....	26
4.2.2 Kujirin Gol .....	31
4.2.3 Prospect 1.....	34
4.2.4 Prospect 2.....	36
4.2.5 Davaa .....	38
4.2.6 Zuukhin Gol .....	40
4.2.7 Prospect 3.....	42
4.2.8 Prospect 4.....	46
4.2.9 Prospect 5.....	48
4.2.10 Mogoin Gol 2 .....	50
4.2.11 Mej Uul .....	52
4.2.12 Undrakh .....	54
4.2.13 Umin Tsagaan Nuu .....	56
4.2.14 Tsookhor Morit.....	58
5 CONCLUSIONS/ RECOMMENDATIONS .....	61
Bibliography .....	59
APPENDIX I: Documentation for the GIS Data Package .....	62

## **List of Figures**

Figure 1.1: Location map of the airborne geophysical surveys in Central – Northern Mongolia. Red Box = Area #01, Blue Box = Area #02, Green Box = Regional Overview from Remote Sensing Imagery. ....	2
Figure 2.1: Factors that affect rock magnetisation (summarised by Isles et al 1998). ....	4
Figure 2.2: Total magnetic intensity reduced to pole (TMI-RTP) image. ....	6
Figure 2.3: First vertical derivative (1VD) of TMI-RTP. ....	7
Figure 2.4: Geophysical data from areas #01 and 02 overlying Landsat 4 TM (bands 741 as RGB respectively) overlying JERS-1/ SAR panchromatic imagery. Note the regional overview available from remote sensing data to assist interpretation of the airborne geophysical survey areas. ....	15
Figure 3.1: Tectonic units of Mongolia (after Sengor et al., 1996) .....	16
Figure 3.2: Idealised model for a porphyry copper deposit and associated magnetic responses (after Clarke et al., 1992). Note that the magnetic response of the system varies with depth of erosion. ....	17
Figure 4.1: Division of the project area into five possible structural and litho-magnetic domains. ....	19
Figure 4.2: Schematic models for the development of the apparent curvilinear character along the Vitim Suture Zone. ....	20
Figure 4.3: Schematic representation of the major structural components that appear to affect domain 3B. ....	22
Figure 4.4: Schematic representation for the development of the major structural components that appear to affect at least domains 2 and 3. ....	23
Figure 4.5: Schematic representation of the major structural components that appear to affect domain 4. ....	23
Figure 4.6: Areas that are considered to contain either structures or intrusive units that could be prospective, particularly for porphyry mineralisation. ....	25
Figure 4.7: Detail around the Erdenetiin Ovoo deposit, (from Dejidmaa and Naito, 1998). ....	26
Figure 4.8: Schematic diagram for the possible evolution of the present low magnetic intensity zone associated with the Erdenetiin Ovoo porphyry deposit. Note the model requires zonation of the granitic bodies and compression between NW trending shear zones. ....	27
Figure 4.9: Characteristics of the Erdenet prospect area. ....	29
Figure 4.10: Schematic end-member models for the possible interpretation for the Kujirin Gol prospect. In reality the true model is likely to represent a combination of both. ....	32
Figure 4.11: Characteristics of the Kujirin Gol prospect area. ....	33
Figure 4.12: Schematic representation of the juxtaposition and alignment of granitic bodies along fault zones, and significant variations in granitic zonation. ....	34
Figure 4.13: Characteristics of the Prospect 1 area. ....	35
Figure 4.14: Schematic representation of the zoned granites within Prospect 2. ....	36
Figure 4.15: Characteristics of the Prospect 2 area. ....	37

Figure 4.16: Schematic representation of zoned multiple phases of early granitic bodies (1, 2 and 3), possibly overprinted by late minor sub-circular intrusive bodies. ....	38
Figure 4.17: Characteristics of the Davaa prospect area.....	39
Figure 4.18: Schematic representation of zoned multiple phases of early granitic bodies possibly overprinted by late minor sub-circular intrusive bodies. ....	40
Figure 4.19: Characteristics of the Zuukhin Gol area. ....	41
Figure 4.20: Schematic representation of a multiple level magnetic response within a basin environment. ....	43
Figure 4.21: Characteristics of the Prospect 3 area.....	45
Figure 4.22: Schematic representation of a small intrusive body within a basin environment. ....	46
Figure 4.23: Characteristics of the Prospect 4 area.....	47
Figure 4.24: Schematic representation of differential strain within domain 3A.....	48
Figure 4.25: Characteristics of the Prospect 5 area.....	49
Figure 4.26: Schematic representation of possible thrusts and truncation of igneous bodies.....	50
Figure 4.27: Characteristics of the Mogoin Gol 2 area. ....	51
Figure 4.28: Characteristics of the Mej Uul area.....	53
Figure 4.29: Schematic representation of radial fracturing around an intrusive body.....	54
Figure 4.30: Characteristics of the Undrakh area. ....	55
Figure 4.31: Characteristics of the Umin Tsagaan Nuun area.....	57
Figure 4.32: Schematic representation of radial fracturing around a possible intrusive body (from Corbett and Leach 1995). ....	58
Figure 4.33: Characteristics of the Tsookhor Morit prospect area. ....	59

## List of Tables

Table 1.1: Datum, projection details for the project and location points of the aeromagnetic survey boundary. ....	1
Table 1.2: Summary of the airborne geophysical survey acquisition parameters.....	1
Table 2.1: A selection of common naturally occurring radioactive minerals.....	10



## **EXECUTIVE SUMMARY**

The project area lies approximately between longitudes 102°20' E and 104°50' E, and latitudes 48°30' N and 49°30' N, and includes a total combined airborne survey area (areas 1 and 2) of approximately 5,665 km<sup>2</sup>.

The focus of this study was to determine the main structural components within the area that could be associated with porphyry Cu-Mo deposits. This work has identified fourteen areas that contain significant structural or litho-magnetic characteristics in association with known mineralisation to be of interest for either unravelling the complex structural history of the area or defining new targets.

From the structural interpretation and litho-magnetic associations it is possible to divide the area into 5 domains. The two most prospective domains are interpreted to be 3A and 2A, as they clearly contain multiple zoned igneous units and are cross-cut by major (E – W and NW – SE trending) regional structures. Domain 3B could contain similar structures to domain 3A, with prospective units at depth, buried by Triassic-Jurassic volcano-sedimentary units.

The predominantly E - W trending structural domain 2A, possibly provides evidence of thrusting having been active in the region which could be beneficial for the development of large porphyry deposits.

Even though structures with an E – W strike appear to be the dominant regional structures (such as the Vitim Suture Zone) this study proposes that the NW trending structures are equally if not more significant for focusing the position of large porphyry mineral deposits.



# 1 INTRODUCTION

The project area lies approximately between longitudes 102°20' E and 104°50' E, and latitudes 48°30' N and 49°30' N, and includes a total combined airborne survey area (areas 1 and 2) of approximately 5,665 km<sup>2</sup>.

The co-ordinates of the airborne survey project areas are shown in Table 1.1. The location of the survey area is presented in Figure 1.1.

Datum and Projection		Easting	Northing		Easting	Northing
World Geodetic Spheroid 84  Universal Transverse Mercator Zone 48		Area #01			Area #02	
	1	390622	5466594	1	325810	5408424
	2	460441	5465657	2	378011	5408063
	3	459971	5398811	3	377687	5391242
	4	398715	5399538	4	325350	5391600
	5	398547	5390325			
	6	389158	5390487			

**Table 1.1: Datum, projection details for the project and location points of the aeromagnetic survey boundary.**

This report provides a summary of the results from the aeromagnetic interpretation component. A separate operations report outlines details of the acquisition and processing (Churchwood, 2001), Table 1.1 provides a brief summary of the main acquisition parameters.

Survey Line Direction	000 – 180 degrees	Tie Line Spacing	2500 metres
Tie Line Direction	090 – 270 degrees	Mean Terrain Clearance	~120 metres
Survey Line Spacing	250 metres	Total Line Kilometres	~25,490 km
Approx. Area Covered	Area #01 = 4,785 km <sup>2</sup> Area #02 = 879.5 km <sup>2</sup>		
Survey Aircraft	Piper Cheyenne PA-31T2 (C-GHRM)		

**Table 1.2: Summary of the airborne geophysical survey acquisition parameters.**

Verification of data quality was undertaken at the base of operations in Bulgan, Mongolia. Final data processing and image processing was carried out at Fugro Airborne Surveys offices in Perth, Western Australia.

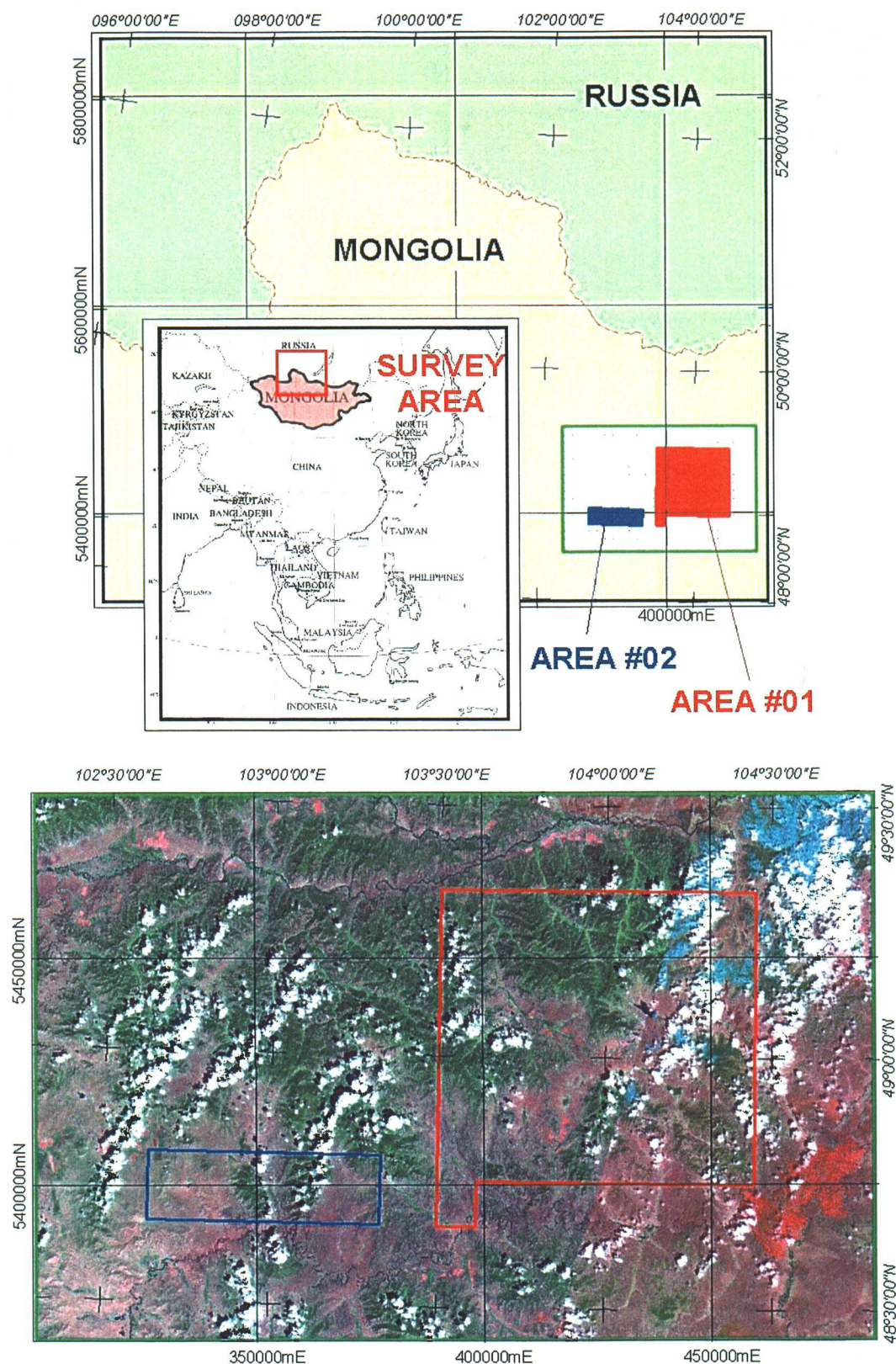


Figure 1.1: Location map of the airborne geophysical surveys in Central – Northern Mongolia. Red Box = Area #01, Blue Box = Area #02, Green Box = Regional Overview from Remote Sensing Imagery.

## 1.1 OBJECTIVES AND PRODUCTS

The project also provides a brief insight to possible mineral targets and prospects from the identification of magnetic characteristics of the multiple intrusive and zoned igneous rocks. The objectives for the interpretation phase are therefore to:

- delineate major and minor structures,
- delineate zones of anomalous radio-element activity that may indicate alteration,
- integrate geophysical data with remote sensing imagery and also published data made available for the project by the clients, in order to assess the region's mineral potential.

The final products from this interpretation include:

- this report which provides a summary of the methodology applied for the interpretation, examples of data from the survey and the results of the interpretation,
- a 1:100,000 'factual' structural geological map in three parts (enclosures 1, 2 and 3) based upon interpretation of the new airborne geophysical data, and integration with remote sensing imagery.
- a 1:250,000 'synthesis' structural geological map (enclosure 4) that summarises the domains and possible fault displacement on the major structures.
- data and interpretation layers compiled in a geographic information system (ArcView™),

These final products provide an indication of the style and extent of geological information that can be gained from the airborne geophysical data. The report also provides examples of the processing, manipulation and interpretation of the geophysical data for the purpose of geological mapping.



## 2 METHODOLOGY AND DATA

All available published geological maps were scanned and geographically rectified to the same projection properties (Table 1.1) as all geophysical data sets and the merged Landsat TM – SAR imagery. Integrated interpretation was achieved through direct on-screen, digital data capture of interpreted geological features, structures and units. Documentation on digital files is provided within Appendix A.

The main focus of the interpretation was on the interpretation of airborne geophysical data from areas #1 and 2. Use of remote sensing imagery enables some consistency between interpretations of the geophysical data and an appreciation of the larger scale structures and distribution of magnetic units.

### 2.1 AIRBORNE MAGNETIC DATA

In a review of aeromagnetic techniques and methodologies, Isles et al (1998) state that “airborne magnetic surveys record variation of the Earth’s Total Magnetic Intensity. In a general sense the Total Magnetic Intensity is directly related to the proportion of magnetic minerals in rocks in the vicinity of the magnetometer. Magnetite is the most common magnetic mineral. Other magnetic minerals of significant abundance are illmenite and pyrrhotite. Factors determining the distribution of magnetic minerals can be grouped into the categories of **primary** and **secondary** processes.

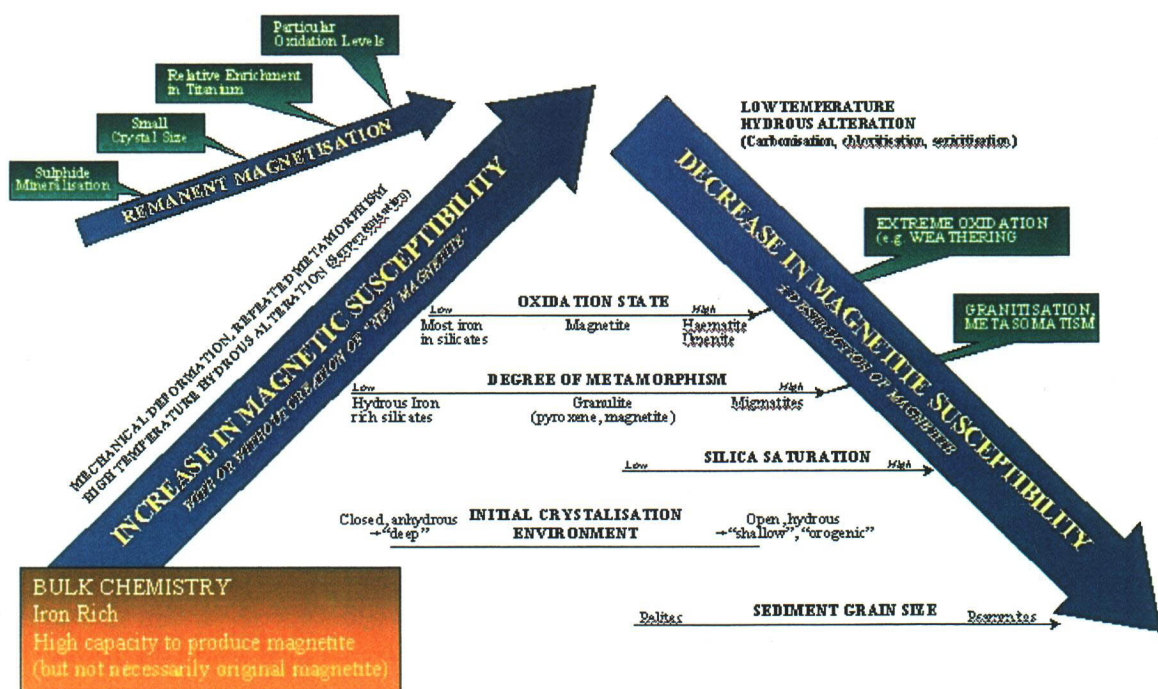


Figure 2.1: Factors that affect rock magnetisation (summarised by Isles et al 1998).

**Primary Controls** on the distribution of magnetic minerals are those that occur during the deposition of sedimentary rocks or the crystallisation of magmas. Volcanic rocks will have different magnetic susceptibilities due to variations in chemistry of the parent magma and differences in geomorphological environments that can influence the rate of cooling. Hence rocks from different episodes of volcanic activity that appear to have a similar lithological character may have subtle variations in their magmatic source and cooling conditions that would result in rocks with different magnetic mineral distributions.

**Secondary Controls** are those that take effect after deposition. These processes can either increase or decrease the amount of magnetic mineral. For example:

- Metamorphism - magnetic susceptibilities of most rocks generally increase with metamorphic grade. However, ultra-metamorphic events such as granitisation generally destroy magnetite.
- Metasomatism – the presence of magnetite or pyrrhotite which allows direct detection of an orebody is often the result of metasomatic alteration of host rocks or precipitation into open space from a fluid.
- Deformation – magnetic susceptibility can be altered by the disruption and reorientation of remanently magnetised material, metasomatism associated with faults, and the effects of grain-scale deformation processes.

All rocks influence the strength of the magnetic field depending on their magnetic properties and proximity to the sensing instrument. Due to the processes described above maps of magnetic intensity can be complex and difficult to interpret. Often, flat-lying volcanic units of differing magnetic character may overlap each other making them impossible to separate, which decreases the likelihood of interpreted lithomagnetic units coinciding with previously mapped surface geology.

#### 2.1.1 Image Processing – Magnetic Data

The image processing of gridded geophysical data for display is very important, as this is the point at which the raw data is transformed into a map which must transfer to the interpreter as much information about the aeromagnetic data as possible. Some common image display methods are described below.

**Total Magnetic Intensity (TMI) Reduced to Pole (RTP) Colour and Greyscale images.**

These images are a direct representation of the magnetic field via variations in either tones of grey or a rainbow colour scheme. They are used to observe absolute changes in magnetic intensity over the region.

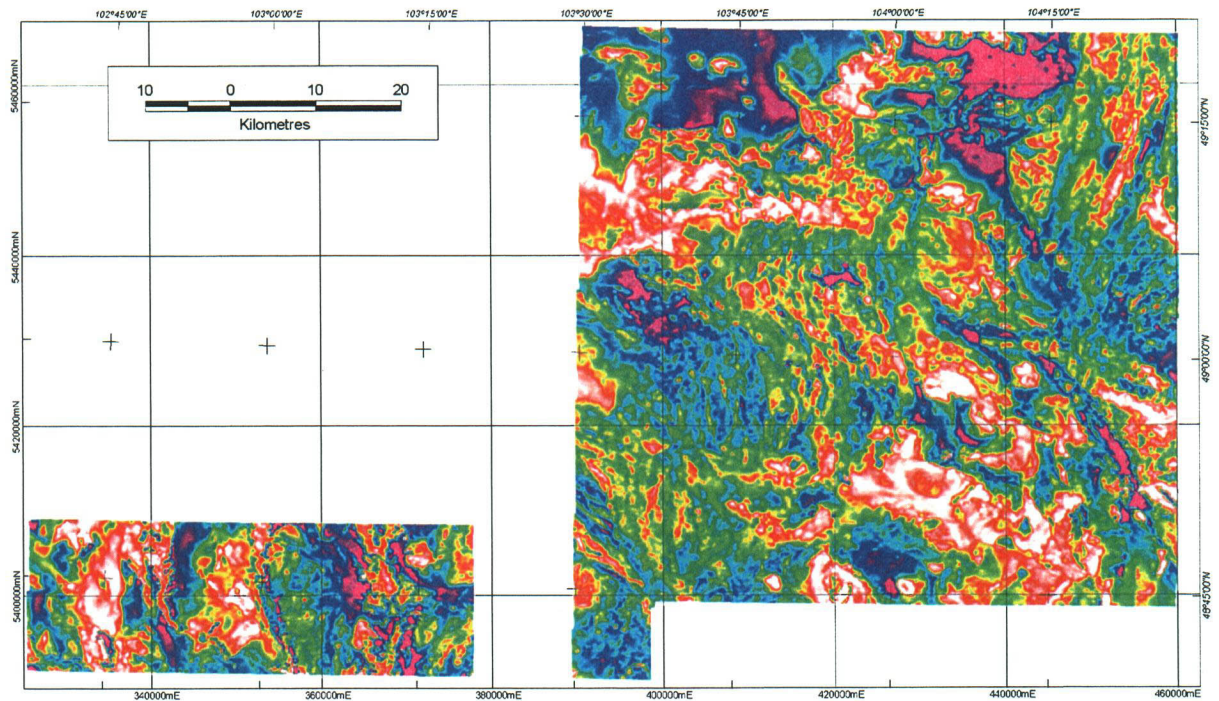


**Figure 2.2: Total magnetic intensity reduced to pole (TMI-RTP) image.**

**First Vertical Derivative (1VD) images of TMI RTP data.** The 1VD image is an approximation of the vertical rate of change of the magnetic field. It tends to enhance the high frequency variations of the magnetic field, and hence is useful for structural mapping, with particular reference to defining faults and lineaments in conjunction with near-surface litho-magnetic boundaries.



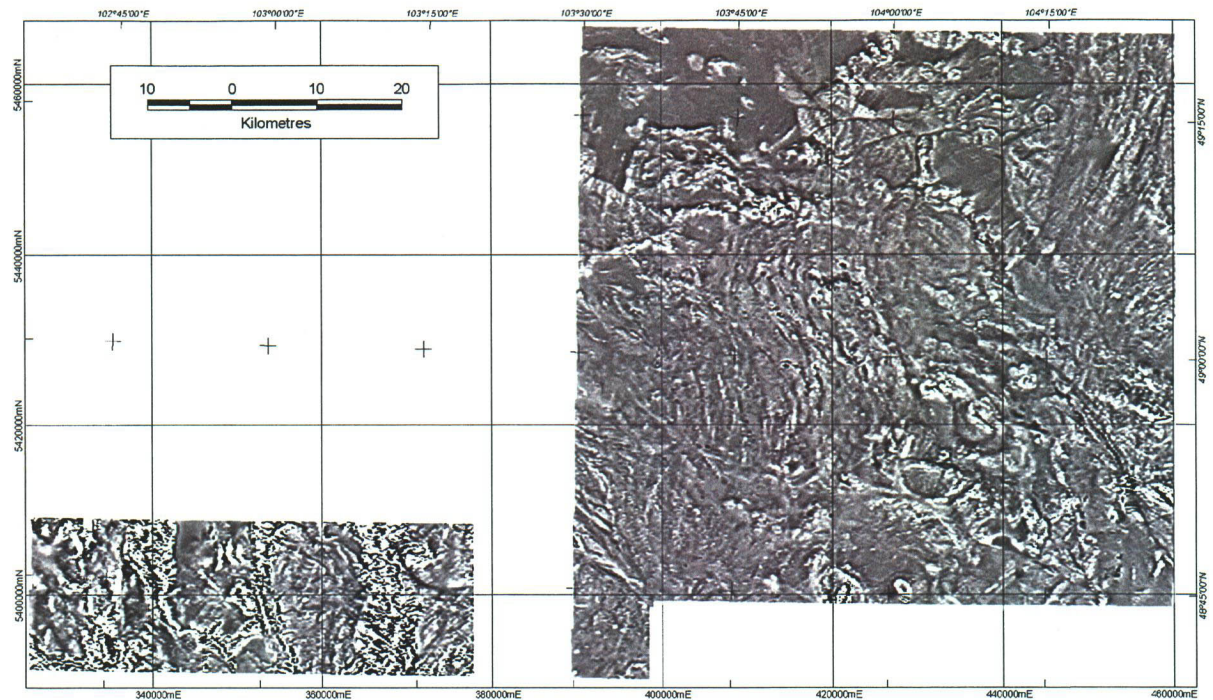


**Figure 2.3: First vertical derivative (1VD) of TMI-RTP.**

**Colour and Grey-scale Second Vertical Derivative (2VD) enhancement of TMI, RTP.**

The 2VD image is approximately a 1VD of a 1VD enhancement. It results in further sharpening the image and enhancement of features with very high spatial frequency. Used as for the 1VD image.

**False Sun Illumination images.** These images are produced mathematically by inferring that the data (magnetics, terrain) represents a 3-dimensional surface that may be illuminated from any direction. Parts of the surface that face the “sun” are illuminated more than those that face away. This accentuates subtle changes in the magnetic field which go unnoticed in a standard grey or colour image. Illumination images enhance features perpendicular to the illumination direction, so several different angles are used.

**Automatic Gain Control Enhancement (AGC, Scale factor = 0.5 and 1.0).** A proprietary in-house filter is applied to the 1VD, TMI, RTP image. This type of imagery attempts to balance anomaly frequencies, subduing high and enhancing weak anomalies. This is particularly useful where there are large variations in the magnetic signature that may otherwise obscure subtle data within the aeromagnetic imagery.



**Pseudo Depth Slices (PDS).** Pseudo-depth slicing (PDS) is a frequency domain filtering technique. It is applied to either total magnetic intensity or reduced to pole magnetic grids. A series of grids that represent different frequency ranges are produced.

The operation attempts to separate magnetic anomalies that have been generated by magnetic source bodies at different depths in the sub-surface. The PDS are derived from an analysis of the log radially-averaged power spectrum, which is a curve that represents the amount of power (amplitude<sup>2</sup>) in each frequency as calculated by the fourier transform. The software and methodology used for pseudo depth slicing is a joint FAS and CSIRO product.

**Digital Terrain Model (DTM).** The digital terrain model is produced by subtracting the ground clearance of the aircraft (recorded by the radar altimeter) from the absolute height recorded by the GPS navigation system. This data is gridded in the same fashion as the magnetic data, and so has the same spatial resolution (50 m cells). The DTM has been used to map faults which affect erosion, and also as the topographic base for 3-dimensional views.

Examples of all these image types are included on the CD accompanying this project.

#### 2.1.2 Influences on Airborne Magnetic Data

Factors such as original pressure and temperature conditions, oxygen availability, environment of deposition, subsequent history of diagenesis, alteration and weathering greatly influence the formation and preservation of magnetic minerals. The degree of magnetisation is not unique. Some geologically distinct formations have similar degrees of magnetisation. Conversely, rock types appearing relatively uniform in mineral composition in the field may display a great variation in degree of magnetisation.

Weathering of the rock surface is likely to have an adverse affect on the magnetic susceptibility value. Measurements of magnetic susceptibility in the field can provide a relative guide as to whether rocks that outcrop cause the magnetic response. A record of the magnetic susceptibility of rock core made as part of the logging procedure would provide useful and accurate data for 3 dimensional analysis and modelling.

Superimposition of anomalies caused by bodies at varying depths may complicate the response. Therefore, it is difficult to directly match surface geological maps with the magnetic data.

### 2.1.3 Uses of Airborne Magnetic Data

The use of airborne magnetic data in the scope of a geological survey is quite broad. The following examples provide an insight into the versatility of magnetic data.

- **Magnetic linear trends** are derived from images that display high frequency information, such as first and second vertical derivatives and pseudo depth slice 1. This layer of the interpretation can be used to indicate bedding or volcanic layering. Inspection of truncations and offsets in the trend data can lead to identification of **faults, fractures** and **folding**. Sense of movement on fault planes can sometimes be deduced from trend patterns.
- **Lithomagnetic Units** comprise geological bodies with uniform and characteristic magnetic signatures. Use of multiple images in the interpretation of lithomagnetic boundaries ensures consistent placement of the boundaries. The units may or may not coincide with previous surface geological map boundaries, as magnetic rocks will affect the measured magnetic field even when buried beneath non-magnetic materials.
- **Intrusive plugs** may appear as isolated sub-circular positive (or negative, if remanently magnetised) magnetic anomalies.
- Buried **intrusive bodies** with a high magnetite content relative to the surrounding rock may appear as broad areas of increased magnetic intensity. It is important to note that the contribution of an overlying magnetic body to the total magnetic intensity can effectively mask the response from buried bodies.
- Regions of generally low or average magnetic intensity and flat texture are often associated with **magnetite destruction** due to injection of alteration fluids, especially where they appear in conjunction with faults and fractures. Flat texture may also be due to the presence of relatively non-magnetic material such as sediment.

## 2.2 AIRBORNE GAMMA-RAY SPECTROMETER DATA

The principles of airborne gamma-ray spectrometer (AGRS) surveys and their application to geological and geomorphological mapping are well established (e.g. Isles et al., 1997, Dickson et al., 1996; Dickson and Scott, 1997; Minty, 1997; Wilford et al., 1997).

It is possible to make a number of generalisations for the AGRS response to various rock types. Typically, there is a progressively higher radioactive response with an increase in acidity of igneous rocks. Consequently, ultramafic rocks tend to produce the lowest AGRS response. Effusive rocks tend to be more radioactive than their deeper equivalents. The radioactive response of sedimentary rocks generally reflects the composition of the original material. The most radioactive sediments are clays, phosphates, potassium salts and bituminous sediments. The least radioactive are limestone, gypsum, rock salt, dolomites and quartzites.

Metamorphic effects on the radioactivity of rocks are usually minimal, with the AGRS response related to that of the original rocks. However, higher metamorphic grades tend to be more variable. The radioactive response from water is typically three or four orders of magnitude less than rock. Exceptions occur when water contains anomalous Rn, Ra or U.

These generalisations can be correlated with the abundance and composition of the different rocks types. Table 2.1 shows some of the radioactive naturally occurring minerals.

Element	Mineral	Occurrence
Potassium (K)	1. Orthoclase and microcline feldspars [ $KAlSi_3O_8$ ] 2. Muscovite [ $H_2KAl(SiO_4)_3$ ] 3. Alunite [ $K_2Al_6(OH)_{12}SO_4$ ] 4. Sylvite, Carnallite [ $KCl$ , $MgCl_2 \cdot 6H_2O$ ]	1. Acid igneous rocks and pegmatites. 2. Acid igneous rocks and pegmatites. 3. Alteration in acid volcanic rocks. 4. Saline deposits in sediments.
Uranium (U)	1. Uraninite [Oxide of U, Pb, Ra + Th, Rare Earths] 2. Carnotite [ $K_2O \cdot 2UO_3 \cdot V_2O_5 + U$ ] 3. Gummite [Uraninite alteration]	1. Granites, pegmatites and vein deposits 2. Sandstones. 3. Associated with uraninite.
Thorium (Th)	1. Monazite [ $ThO_2$ + Rare earth phosphate] 2. Thorianite [(Th, U) $O_2$ ] 3. Thorite, Uranothorite [ $ThSiO_4 + U$ ]	1. Granites, pegmatites and gneiss. 2 & 3. Granites, pegmatites and placers

**Table 2.1: A selection of common naturally occurring radioactive minerals**

Within any given rock-type, there is a wide range of values (Killeen, 1979, Fertl, 1983). Consequently, no global classification of rock type by radioelement content alone is possible with any level of certainty.

### 2.2.1 Image Processing – Gamma-ray Spectrometer Data

A range of imagery can be produced (for example Wilford *et al.*, 1992). Interpretation of AGRS data from the district-scale study area made use of a series of images that include:

**Ternary Images** – combination of K (red), Th (green) and U (blue) data. Low response in all channels appears as black (e.g. over water), while high relative response in all channels appears as white. Intermediate colours represent variations in the channels.

In regions of good outcrop or in arid climates where vegetation is less dominant, the various channels of AGRS data can be used to accurately map changes in surface lithology. However, the ternary image does not provide a quantitative representation of the radioelements, instead reflecting relative variations in radioelement distribution.

**Individual K, Th, U and Total Count images.** These images were used to map lithological boundaries. They provide information that may not be visible in the combined image. May be used to map alteration zones if K enrichment, or significant quantities of U or Th mineralisation are present.

**Clipped Images.** These images are typically individual K, Th and U images that only display the user-defined upper limit (typically the uppermost 5%, 10%, 15%, 20%, 30% and 45%) of the radiometric count. The objective of clipping the data to the highest total range is to delete much of the background noise and so assist in the determination of mappable boundaries or the identification of major anomalous zones.

**Ratio Images.** These images enable the visualisation of subtle changes between two gamma-ray responses that occur due to variations in the mineral chemistry of the host rock that may not be evident in single images. Constructed by dividing the response in one band by that in another, e.g. K/ Th.

**Composite Images** include radiometric ternary or single channel data merged with another data source. Typical data to merge with radiometric information include Digital Elevation Models (DEM), Remote Sensing (eg greyscale Landsat TM, Aerial Photographs) and magnetic data.

## 2.2.2 Influences on Airborne Gamma-ray Spectrometry

A large variety of naturally occurring geological, geochemical and geomorphic processes influence the distribution of individual radionuclides. Other factors that can influence the levels of gamma-radiation recorded are simply a result of the instrument quality and survey acquisition parameters:

- Various estimates suggest that the majority of gamma-rays emissions are from the top 10 to 50 cm of rock or soil. Hence weathering of in situ rock, erosion and transportation can have a significant effect on measured radiation levels. For example, a thin layer of colluvial or alluvial material can completely mask the AGRS response of the underlying bedrock.
- Unless there are detectable differences in composition between lithological units, and these differences are retained in surficial materials, the method can not be effective for lithological mapping. Where surface material consists of impermeable transported alluvium, lacustrine or marine silts or clays, clay till or aeolian sand, the method can only indicate the geochemistry of these materials and not that of the underlying bedrock.
- The measured level of radiation intensity decreases exponentially with flying height. This may result in abnormal changes of signal over the crests of hills and bases of valleys where the aircraft height is likely to vary most from the specified survey altitude.
- The presence of water can severely attenuate gamma-rays. Water-covered areas will exhibit little or no gamma radiation signal. Dry soil conditions, or at least relatively constant soil-moisture conditions are preferable for flying AGRS surveys. Vegetation can attenuate the signal depending on the density of cover, due to water content of the plant material. In some instances, the uptake of potassium by plants can contribute to the measured signal. This may sometimes reflect the potassium abundance of the sub-surface rocks.
- The AGRS detector uses a swathe not a point source. The detection interval is variable dependent on survey parameters. Recordings are accumulated over the entire pre-determined interval, eg 70 m. Depending on distribution, sampling width and imaging criteria several points with relatively similar values may combine to form a broad anomaly.
- Survey design - The footprint of the sensor is determined by the flying height of the aircraft, as well as its ground speed. Decreasing flying height will not only increase the amount of radiation detected (and hence data quality), but also reduce the area on the ground from which the signal originates i.e., increase spatial resolution. Decreasing aircraft speed will also increase spatial resolution by reducing the area covered in each recording period (usually 1 second intervals [1 Hz] representing a distance of about 70 m

between readings at ground level). Generally, AGRS data is of secondary importance, as the survey is usually designed with airborne magnetic data as the focus. Airborne magnetic data is more closely spaced with data recorded at 0.1 second intervals (10 Hz), representing about 7 m separation at ground level. Safety issues also take priority over optimum survey specifications.

### 2.2.3 Uses of AGRS Data

The use of AGRS data in the scope of a geological survey is quite broad and its effectiveness is variable. Some of the more typical uses are:

- Differentiation of the petrographic composition of intrusive, effusive and crystalline rock complexes.
- Delineation of intrusive rocks inside surrounding units formed by sedimentary or metamorphic complexes (mapping borders).
- Differentiation of various types of xenoliths inside intrusive rock bodies.
- Mapping suites of pegmatite veins and dykes that accompany intrusive bodies and the delineation of small intrusive bodies and their derivatives.
- Mapping zones of alteration.
- Mapping sedimentary lithological and facies variations.
- Assist stratigraphic and structural-tectonic studies by mapping radioactive horizons.
- Study of the structural-tectonic properties of intrusive, effusive and crystalline complexes.

The mapping and alteration detection capabilities of AGRS data are applications that are achievable as stand alone interpretative products. The tectonic and structural interpretation applications however, usually require integration with other data.

Airborne GRS surveys can be of direct assistance to exploration for many commodities, most obviously U and Th, but also Sn, W, REE, Nb and Zr. Less often, but of importance in specific circumstances, AGRS anomalies can point to Au, Ag, Hg, Co, Ni, Bi, Cu, Mo, Pb and Zn mineralisation. Mineralisation is detected either because one or more of the radioelements is an associated trace constituent or because the mineralising process has changed the radioelement ratios in the surrounding environment.

Unless there are detectable differences in composition between lithological units, and these differences are retained in surficial materials, the method can not be effective for lithological mapping. Wherever surface material consists of impermeable transported alluvium, lacustrine or marine silts or clays, clay till or aeolian sand, the method can only indicate the geochemistry of these materials and not that of the underlying bedrock.

During weathering, destruction of the major K hosts occurs in the order biotite → K-feldspar → muscovite. The formation of K-bearing minerals such as illite may take up Potassium released during weathering. Under suitable conditions, it can also be adsorbed in minor amounts into other clays, such as montmorillonite. The efficient uptake of K by clays is reflected in the low concentration of K in seawater (380 ppm).

Of the major U-bearing minerals, only zircon and monazite are stable during weathering. Authigenic iron oxides and clay minerals may retain uranium freed by the breakdown of minerals during weathering. Alternatively, precipitation of uranium under reducing conditions may form deposits in favourable circumstances.

Thorium freed by the breakdown of minerals during weathering may be retained in Fe or Ti oxides, hydroxides and clays. Thorium may also be transported and adsorbed in to colloidal clays and iron oxides.

Usually K tends to be mobile during weathering compared to U and Th. However, silicification can preserve shale units near the surface in weathering regimes, resulting in K and Th-rich areas that correspond to topographic highs. The retention of U and Th, but loss of K, can result in distinct AGRS signatures for argillic units.



### 2.3 LANDSAT TM

Both Landsat TM and JERS-1/ SAR radar imagery were provided by the client and used by Fugro Airborne Surveys for the project area. The Landsat 4 TM imagery was merged and ortho-rectified using standard 1:500,000 topographic maps and locally improved by additionally rectifying using the digital topographic data acquired from the geophysical survey (Figure 2.4). Images used were:

Landsat 4 TM path/row 134/26, acquired 19<sup>th</sup> August 1989,

Landsat 4 TM path/row 133/26, acquired 9<sup>th</sup> June 1989,

For details of the JERS-1/ SAR imagery refer to the report by JICA and MMAJ, 2001. The sheets most relevant to this study include; Mutag, Ingettologoy, Jagalant and Bulgan.

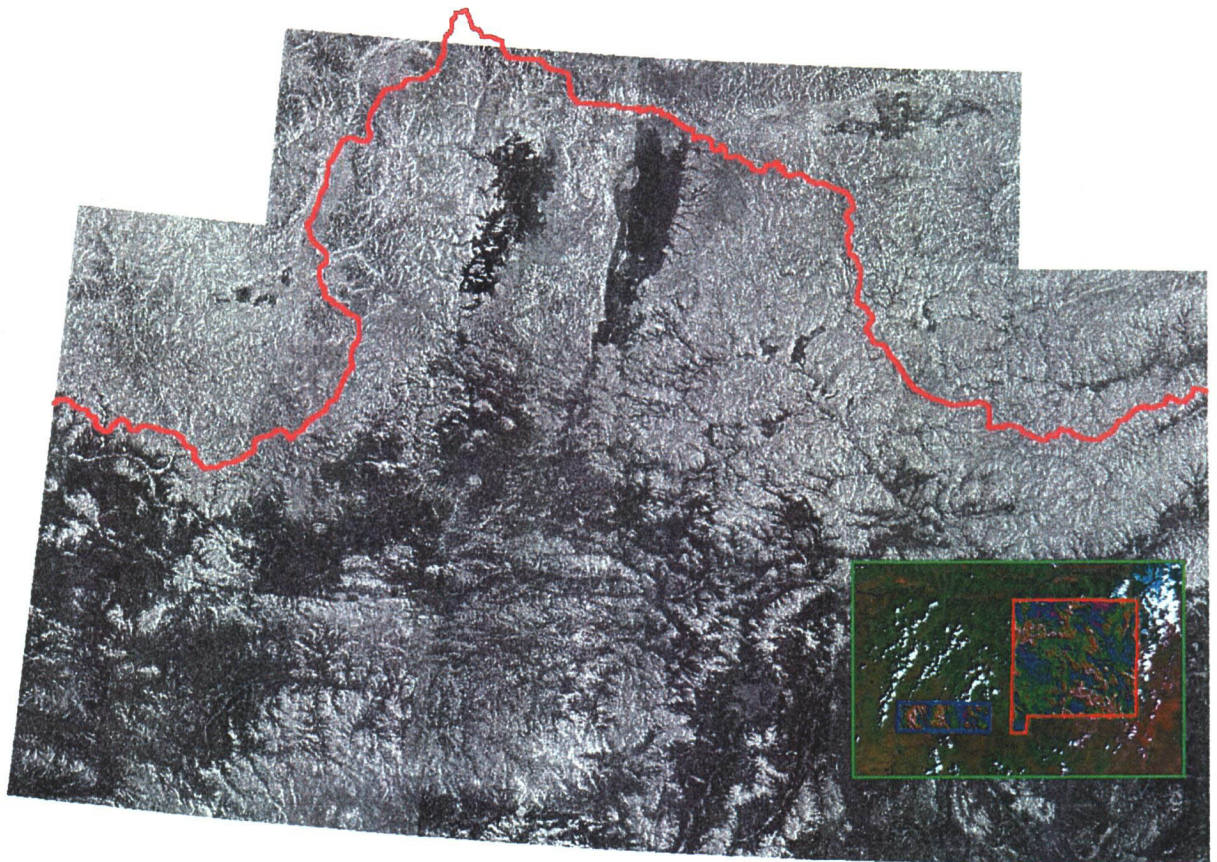


**Figure 2.4: Geophysical data from areas #01 and 02 overlying Landsat 4 TM (bands 741 as RGB respectively) overlying JERS-1/ SAR panchromatic imagery. Note the regional overview available from remote sensing data to assist interpretation of the airborne geophysical survey areas.**



### 3 GEOLOGY REVIEW

A comprehensive review of the geology of the region of central north Mongolia has been undertaken by JICA and the MMAJ (2001). Other significant references from which to review the general geology of the area are Jargalsaihan et al (1996) and Sengor et al (1996). This section only aims to briefly emphasise some of the key points relevant to this study of the West Erdenet Area. A comprehensive review is beyond the scope of this study.

The main unit that is of interest to this study is the Tuva-Mongol Unit **FIGXX**. A small portion of the Khangay-Khentiy Unit may crop out in the SE of the study area and is also described.

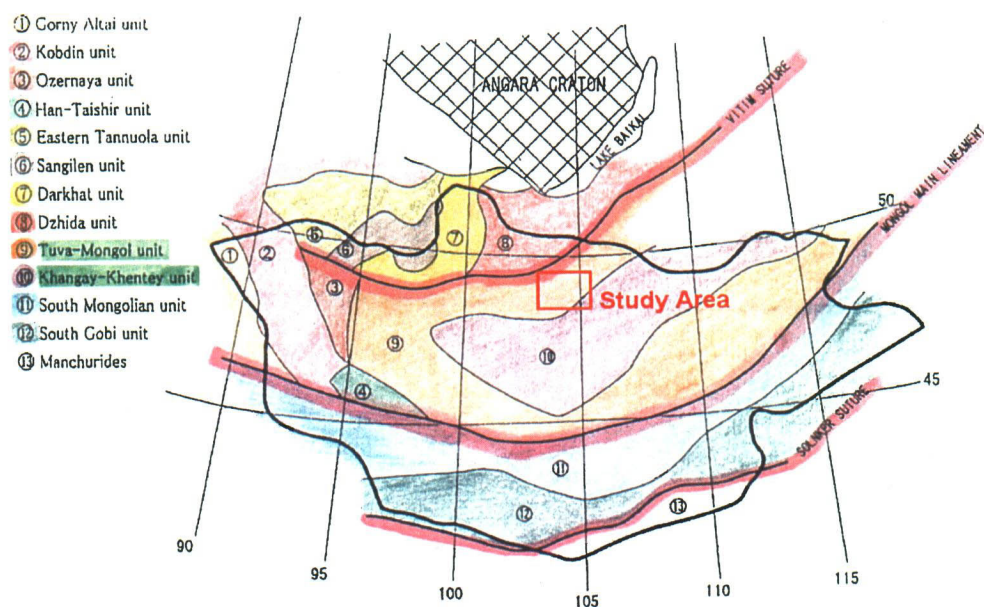


**Figure 3.1: Tectonic units of Mongolia (after Sengor et al., 1996)**

The JICA and MMAJ (2001) describe these units as:

- **“Tuva-Mongol Unit** consists of continental crust before the formation of the Altai and magma arcs of the Vendian to Permian. The continental crust which is the basement of the island are consists of migmatite, granite, anorthosite and granulite, that is similar to the Angara craton. The island are basement is intruded by granite of  $2,364 \pm 6$  Ma. This consists of high-grade metamorphic rocks of the Archaean which was separated by ophiolite of the Vendian to early Cambrian and island arc volcanics of the Riphean. The basement is covered by shelf limestone of the Vendian to Cambrian. Clastic rocks of the early to middle Palaeozoic and granites of the Palaeozoic distribute over a wide area. Syenite of the Devonian to Permian, calc-alkaline rocks of the Devonian, and calc-alkaline and alkaline rocks of the Permian occur. About the origin of this unit, it is said

that micro-continents gathered to form the Tuva-Mongol micro-continent and subduction zone developed at its margin and accretionary prism and magma arcs occurred”,

- **“Khangay-Khenti Unit** consists of accretionary prism and magma arcs. This consists of ophiolite, serpentinite melange, chert, limestone and shale of the late Riphean to early Cambrian as well as turbidite, basic to intermediate volcanic rocks, tuff and chert of the early Palaeozoic to Carboniferous, and turbidite, gabbro and basalt of the Carboniferous to Triassic. This shows a shape of horseshoe opening toward the northeast and consists of a few island arc units which are folded and stacked. The respective units show the age polarities of getting younger toward the northeastern side. These are intruded by granites of the Permian, Triassic and Jurassic”.

Gunn and Dentith (1997) review porphyry deposits with a particular emphasis on the geophysical response and state that,

“the term porphyry copper deposit encompasses the Cu, Cu-Au and Cu-Mo deposits associated with intrusive stocks of generally felsic and porphyritic nature, emplaced above down-going plates in island arc or Andean settings (Sawkins 1990). The mineralisation occurs as veins and disseminations in country rock above and adjacent to the upper portions of intrusions and in the upper parts of intrusions themselves. Systematic radial zoning of

mineralisation and alteration has been identified in the majority of such deposits and a series of models for such zonings have been published. Figure XX shows a generalised representation of zoning in a porphyry system.

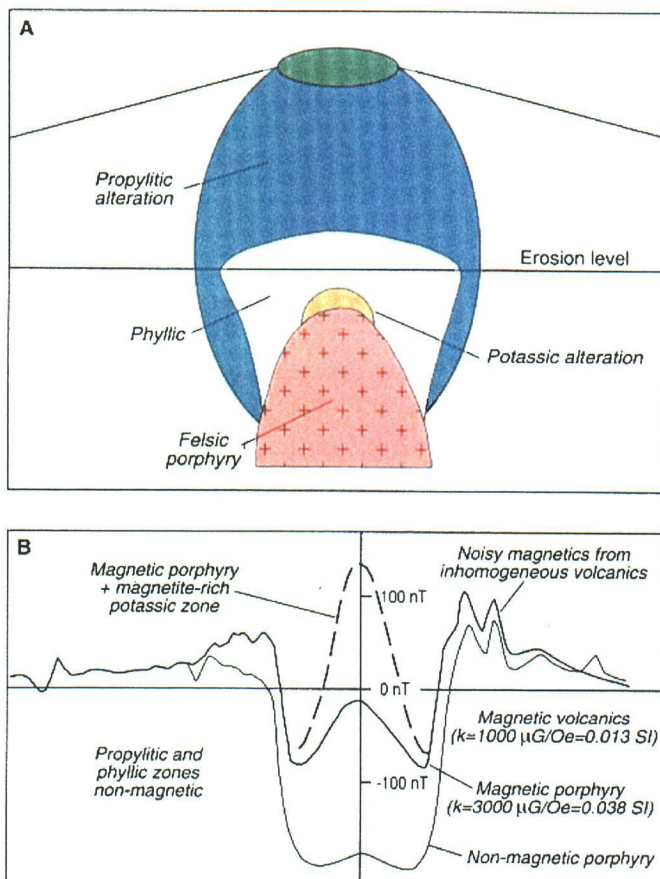


**Figure 3.2:** Idealised model for a porphyry copper deposit and associated magnetic responses (after Clarke et al., 1992). Note that the magnetic response of the system varies with depth of erosion.

As discussed by Clark et al (1992), such intrusive systems have a semi-predictable magnetic response, albeit one related to the depth of erosion of the system. Fig xx incorporates an idealised magnetic profile for a vertical inducing field (i.e. there is no distortion due to field inclination) reproduced from Clark et al 1992), for the erosion level indicated in the figure.

Typically, such intrusive systems are emplaced in volcanics or are capped by volcanics associated with the intrusion. The volcanics, which are routinely inhomogeneous in nature, provide an erratic high-level magnetic response to the area. Destruction of magnetite in these volcanics by propylitic and phyllic alteration can cause a smooth broad magnetic low over the vicinity of the intrusion. The felsic porphyry is generally, but not always, ferromagnetic in nature and, in such cases, a sharp localised magnetic high can occur in the centre of the magnetic low. This model produces a signature of porphyry copper deposits that is not directly related to the mineralisation, but rather to the ensemble of geology and processes associated with the formation of the mineralisation. Brant (1966) has published results of an aeromagnetic survey over the Bagdad porphyry copper deposit in Arizona, which appears to fit this model".